

# Analysis of 6(4) - Valued Memory

M. Guzan<sup>1</sup>

<sup>1</sup>*Department of Theoretical and Industrial Electrical Engineering, Faculty of Electrical Engineering and Informatics, Technical University of Kosice, Park Komenského 3, 042 00, Kosice, Slovak Republic  
milan.guzan@tuke.sk*

**Abstract**—The subject of the article is an analysis of multiple-valued memory, which, according to previously verified assumptions should contain up to 6 stable singularities and an unspecified number of undesirable stable limit cycles. Eigenvalues, however, suggested that instead of 6 stable singularities, the memory is characterized by only four of them. This fact was verified initially by trajectories and consequently also by the calculation of boundary surface section led exclusively through the “suspicious” singularities. The result of the analysis is probably the first reference of violated alternation of stable and unstable singularities in sequential circuit.

**Index Terms**—Differential equations, memory, multilevel systems, sequential circuits.

## I. INTRODUCTION

Although binary logic is dominant nowadays, multiple valued logic (MVL) is still of interest as well. Advantages of MVL compared with binary logic, according to [1] are indisputable: reduced number of circuits providing transfer to higher orders, increased integration density and reduced volume of arithmetic operations. The timeliness of circuits using MVL is also confirmed by U.S. Patent [2], and by recently published work [3]–[5].

Multiple-valued (MV) memory can be created either using CMOS transistors, or by resonant tunneling diodes (RTDs), or by combination of one CMOS transistor and one RTD. Analysis of CMOS MV memories was no problem [6], [7]. Circuits were characterized by such number of attractors, which corresponded to the number of stable singularities in the circuit. Similarly, the analysis of elemental MV memory consisting of two RTDs connected in series (Fig. 1) indicated equal number of attractors or attraction regions, and the number of stable singularities. Parameters related to parasitic capacitance and inductance ( $C_1$ ,  $C_2$  and  $L$ ), however, did not correspond to the actual values on the chip.

They were much larger. After approaching the real values of the parasitic  $L$ ,  $C_1$ ,  $C_2$  on the chip, the authors of the work [8] found in the ternary memory not only three regions of attractiveness for static attractors (for three stable singularities), but also other undesirable dynamic attractor – a stable limit cycle (SLC). Corresponding to this was forth region of attractiveness in the appropriate projection plane. Its presence made the MV memory dysfunctional and authors became interested in the impact of negative differential resistance (NDR) area on MV memory and SLC existence.

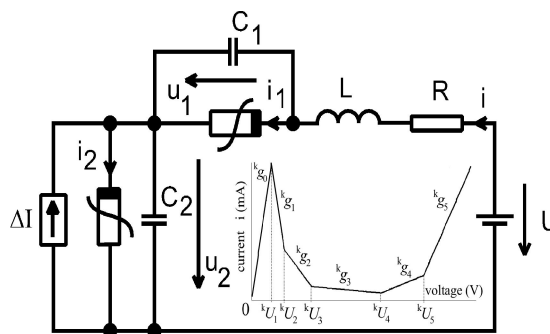


Fig. 1. Model of the elementary memory cell.

Since until then, only cases of autonomous circuits were analysed, with the load with positive differential resistance (PDR) [6], [7], [9]–[14], no unwanted SLCs were observed. In the following period, results of analysis with real parasitic parameters on chip for the three-valued memory [15]–[18], four-valued memory [19] and five-valued memory [20] were published. The object of this paper is to analyse the six-valued elemental memory formed of two RTDs connected in series.

## II. MULTIPLE-VALUED ELEMENTAL MEMORY

The analysed MV memory is illustrated in Fig. 1 and the circuit is described by the system (1):

$$\begin{cases} L(di/dt) &= U - Ri - (u_1 + u_2) &\equiv Q_1, \\ C_1(du_1/dt) &= i - f_1(u_1) &\equiv Q_2, \\ C_2(du_2/dt) &= i - f_2(u_2) + I &\equiv Q_3, \end{cases} \quad (1)$$

where the characteristics of nonlinear elements  $f_k(u_k)$  according to [21] are defined by (2) where  $g_k$  are conductivities of the  $k$ -th element and  $U_k^v$  are breakpoints of the  $v$ - $i$  characteristic shown in Fig. 1. If  $k = 1$  it is a load, if

Manuscript received October 3, 2013; accepted February 24, 2014.



We support research activities in Slovakia / Project is co-financed from EU funds. This paper was

developed within the Project "Centre of Excellence of the Integrated Research & Exploitation the Advanced Materials and Technologies in the Automotive Electronics", ITMS 26220120055

$k = 2$  it is the element. For too long relation (2) expressing piece-wise linear (PWL) characteristic of element and load, we list the relation with beginning and end indexes. Then, other missing elements can be easily added. Capacitances  $C_1, C_2$  include the capacitance of the equivalent circuit of elements, or parasitic capacitance on the chip. Inductance  $L$  is the inductance of inputs to the elements and resistor  $R$  expresses resistance of conductive connections on the chip. Supply voltage is  $U = 440$  mV and in the next we consider control pulse  $I = 0$  and  $R = 0$ . Parameters of both RTDs are equal and listed in Table I.

$$f_k(u_k) = \frac{1}{2} \left( {}^k g_0 + {}^k g_4 \right) u_k + \frac{1}{2} \left[ \left( {}^k g_1 - {}^k g_0 \right) \left| u_k - {}^k U_1 \right| + \left( {}^k g_2 - {}^k g_1 \right) \left| u_k - {}^k U_2 \right| + \dots + \left( {}^k g_5 - {}^k g_4 \right) \left| u_k - {}^k U_5 \right| \right] - \frac{1}{2} \left[ \left( {}^k g_1 - {}^k g_0 \right) {}^k U_1 + \left( {}^k g_2 - {}^k g_1 \right) {}^k U_2 + \dots + \left( {}^k g_5 - {}^k g_4 \right) {}^k U_5 \right]. \quad (2)$$

TABLE I. PARAMETERS OF RTDS.

$i$	0	1	2	3	4	5
$g_i$ (S)	0,3	-0,3	-0,06	-0,004	0,018	0,1
$U_i$ (mV)	-	40	65	120	260	345

The number of singularities is defined by the right-hand sides of the (1) and the locations of the singularities (coordinates, see Table II) are given by the system of algebraic equations

$$Q_1 = Q_2 = Q_3 = 0. \quad (3)$$

The corresponding memory cell in Fig. 1 has 11 singularities. For better orientation, second part of Table II lists conductivities, which form corresponding singularity. Graphical representation of projection of the  $v$ - $i$  characteristics of RTDs (element - solid line, load - dashed line) and singularities in the plane  $i, u_2$  is shown in the Fig. 2.

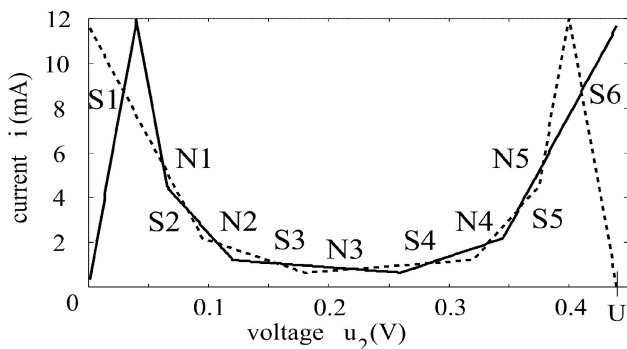


Fig. 2. Projection of the PWL  $v$ - $i$  characteristics (element is solid line and load is dashed line) and depiction of the singular points into the plane  $i, u_2$  for  $R = 0$ .

In binary or MV memories analysed so far, the regularity of alternation of singularities was *always* in effect: stable–

unstable–stable etc. (S–N–S etc.) while the first and last singularities must be stable. Designation S1–S6 or N1–N5 then implies that under the assumption there is the stable (S) or unstable (N) singularity and so the author of the article considered this memory structure as six-valued. However, the stability or instability of singularities is decided by eigenvalues of the Jacobian matrix. The eigenvalues corresponding to singularities are listed in Table III.

It shows obviously that the memory, which appeared as six-valued at the beginning of this analysis, is actually only four-valued (!), because eigenvalues corresponding to S2 and S5 (in comparison with eigenvalues S1, S3, S4 and S6) have only  $\lambda_1 < 0$  and  $Re\{\lambda_{2,3}\} > 0$ . Moreover, also other unstable singularities are interesting, because although N1 and N5 are classic saddle-type point ( $\lambda_1 > 0, \lambda_2 < 0, \lambda_3 < 0$ ), but N2, N3 and N4 have eigenvalues  $\lambda_1 > 0$  and  $Re\{\lambda_{2,3}\} > 0$ !

TABLE II. COORDINATES OF ALL 11 SINGULARITIES.

	$u_1$ (mV)	$u_2$ (mV)	$i$ (mA)	${}^1 g_i$ (S)	${}^2 g_i$ (S)
<b>S1</b>	410	30	8,75	0,1	0,3
<b>N1</b>	378	62	5,51	0,1	-0,3
<b>S2</b>	358	82	3,5	0,1	-0,06
<b>N2</b>	332	108	1,94	0,018	-0,06
<b>S3</b>	283	157	1,05	0,018	-0,004
<b>N3</b>	220	220	0,8	-0,004	-0,004
<b>S4</b>	157	283	1,05	-0,004	0,018
<b>N4</b>	108	332	1,94	-0,06	0,018
<b>S5</b>	82	358	3,5	-0,06	0,1
<b>N5</b>	62	378	5,51	-0,3	0,1
<b>S6</b>	30	410	8,75	0,3	0,1

TABLE III. EIGENVALUES OF ALL 11 SINGULARITIES.

	$\lambda_1$	$\lambda_{2,3}$
<b>S1, S6</b>	-1121065246658,71	-208698145901,41±96055537292,46i
<b>N1, N5</b>	1120279841165,22	-109195285224,98; -241853786709,47
<b>S2, S5</b>	-275071570315,14	60612708234,49±133556900772,98i
<b>N2, N4</b>	112134460619,92	24702000459,27±234086876479,59i
<b>S3, S4</b>	-27564330336,67	-13140911754,74±273789816718,72i
<b>N3</b>	15384615384,62	7692307692,31 ±277243404476i

Thus, in one memory structure we get several types of unstable singularities (moreover, in the case of N1 and N5 without imaginary part - all other eigenvalues of singularities have complex conjugate root  $\lambda_{2,3}$ ), which is quite unusual and surprising.

Therefore, based on Table III, we can conclude that instead of 6 stable singularities in Fig. 2, the memory is characterized by only 4 stable singularities – i.e. S1, S3, S4 and S6. All other singularities (total 7) are unstable singularities. Just commented case is probably the first case, which at  $R = 0$  distorts the regularity of alteration of singularities S–N–S etc. At the same time, following questions arise: 1. What caused the violation of mentioned alteration of singularities? 2. How will the presence of only 4 stable and up to 7 unstable singularities influence the boundary surface (BS) morphology? 3. How does the NDR

region impact the change of singularity character? The first and third issue will be subject of the following activities of the author, the second question will be answered in the next part of this paper.

### III. BOUNDARY SURFACE OF THE MV MEMORY

When designing new memory structure, one should answer the question of reliable control of MV memory.

The parameter of controlling  $I$  impulse cannot be exactly determined without knowing the BS. Determination of  $I$  parameters was introduced in [22]. Of course, a prerequisite for reliable control of MV memory is the absence of SLC. However, even when SLC occurs, it makes a difference to know the BS both in terms of its morphology, and in terms of the circuit theory. Moreover, the incidence of unstable singularities with positive eigenvalues is also interesting in system (1) by backward integration [17]. Unstable singularities S2 and S5 can be verified in two ways:

a) By entering IC close to S2 or S5 and tracking the movement of representative point (RP). If S2 or S5 are not attractors, singularities are unstable;

b) By calculating the cross-section of BS.

Verification by point a) was positive - RP always went away from S2 or from S5 and was never attracted by S2 and S5 "attractor". For verification by point b) it holds that if the mentioned singularities are really unstable, then the BS must pass through both singularities. As the current level for S2 and S5 is the same ( $S2, S5i = 3.5$  mA), one cross-section of BS will be sufficient for instability verification.

The algorithm for calculating the cross-section of BS is as follows:

1. Projection plane is divided into  $M \times N$  points. These will be like initial conditions (ICs) for solving the system (1), e. g. by Runge-Kutta method;

2. For the selected IC, in solving the system (1) it is evaluated by which attractor the RP will be attracted;

3. The result of calculating the net of  $M \times N$  points - ICs, is a text file that contains coordinates of IC ( ${}^{IC}i, {}^{IC}u_1, {}^{IC}u_2$ ) and a numerically labelled attractor. If colour is attributed to each attractor, graphical output of a text file will be coloured mosaic of regions of attraction for individual attractors.

By applying the above mentioned procedure of calculating BS cross-section, Fig. 3(b) shows the calculated cross-section of BS in the plane  $u_1, u_2$  for  $i = 3,5$  mA, parameters listed in the Table I and Table IV.

TABLE IV. PARASITIC PARAMETERS FOR MEMORY CELL IN FIG. 1.

$L$ [H]	$C_1 = C_2$ [F]	$R$ [ $\Omega$ ]
1.10-10	2,6.10-13	0

In total, the picture consists of  $440 \times 440$  points (ICs), which represents calculation of 193 600 trajectories.

The key to understanding Fig. 3(b) and later commented Fig. 3(d) is as follows:

Symbols  $\bullet$  or  $+$  correspond to stable (S1, S3, S4 a S6), or unstable (N1, N2, N3, N4 and  $*S2, *S4$ ) singularities. Colour scale (or grey scale when printing in grayscale) of attraction regions corresponds to the location of descriptions of singularities S1, S3, S4 and S6 and SLC L1–L9 in colour

areas, so e.g. the region of attraction for S3 is blue and the region of attraction for SLC L8 is yellow. Although SLC L8 is also blue, as the region of attraction for S3, L8 marking in the corresponding region clearly distinguishes both areas from each other. Diagonal black line, on which the symbols  $\bullet$  and  $+$  lie, represents the projection of  $v-i$  RTDs characteristics to the projection plane  $u_1, u_2$  for  $R = 0$ . Similar comment applies also for Fig. 3(d).

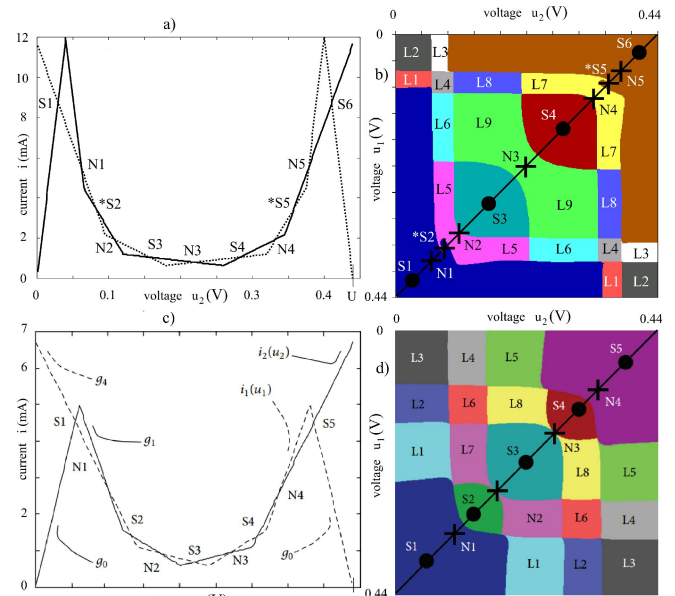


Fig. 3 Comparison of two similar MV memories after an unexpected reduction of the number of stable singularities: (a) or (c) Projection of the PWL  $v-i$  characteristics (element is solid line and load is dashed line) and depiction of the singular points into the plane  $u_1, u_2$  for  $R = 0$ , for parameters: (3) or those mentioned in [21]; (b) or (d) Cross-sections of the BS in the plane  $u_1, u_2$  for:  $*S2, *S5i = 3,5$  mA resp.  $N2, N3i = 0,94$  mA. Values of the parasitic elements considered in both simulations as mentioned in (7).



Fig. 4. Details of  $*S2$  and  $*S5$  surroundings. Without  $+$  symbol the BS "tail" is clearly visible around singularities. Diagonal white line is the projection of RTDs characteristics in a plane  $u_1, u_2$  for  $R = 0$ .

Figure 3(a) and Fig. 3(c) thus show PWL characteristics as the element and load for the structure analysed in this article, or for the structure analysed in [20]. Figures 3(b) and Fig. 3(d) illustrate the morphology of BS, which is very complex by SLC. Although the singularity S2 is in both cases formed by the third segment of element (with NDR) and by the last segment of load (with PDR), nevertheless the structure in Fig. 3(a) shows violated alteration S–N–S etc., and S2 becomes unstable singularity. To avoid the notion that S2 is a stable singularity (as opposed to picture in Fig. 2), we change identification of the S2 to  $*S2$ , see Fig. 3(a), Fig. (b). Similar comment applies to S5. The fact that  $*S2$  or  $*S5$  is really unstable, is documented in Fig. 3(b). It is a cross-section of BS in the plane  $*S2, *S5i = 3,5$  mA (see Table II). As seen from Fig. 3(b), the  $+$  symbol is located at the boundary of regions of attraction for S1 and L5 or S6 and L8. As Fig. 3(b) is graphically edited, detail of  $*S2$  or  $*S5$  surroundings is illustrated in Fig. 4. In

this view, also the "tail" of BS is of interest, which is not observed at any colour region in Fig. 3(b). Cross-section of BS in Fig. 3(b), however, does not provide information on the 3D size of particular regions of attraction.

To get a comprehensive idea, it would be necessary to calculate around 15–30 BS cross-sections for different current levels, similarly as it was done in [20]. However, this will be the subject of future activities, partly because calculating the BS cross-section in Fig. 3(b) took about 8 hours, while using all 4 CPU cores of the PC (PC Specifications: Intel Core2 Quad CPU 2.84 GHz, 4GB RAM).

When using only one CPU core, the calculation of one BS section would last about 30 hours, which places great demands on computing power.

Figure 3(d) illustrates a view of BS cross-section for unstable  $N_2$  and  $N_3$  for  $N_2, N_3 i = 0,94$  mA and the parameters in Table IV. The parameters for RTDs can be found in [20] in (5). Because the character of singularities did not change in this structure, regions of attraction are more evenly distributed in state space than in Fig. 3(b). One can get an idea of the size of different areas in the 3D state space after seeing a series of BS cross-sections for the planes from  $i = -12$  mA to  $i = +15$  mA (Fig. 7 in [20]).

#### IV. CONCLUSIONS

The paper presents an analysis of a structure similar to one that has already received publicity in [20]. PWL  $v-i$  characteristics of RTDs were enriched by one segment, which increased the number of singularities from 9 to 11. As in the similar structures of MV memories at the same parasitic parameters (7) was found the incidence of undesired SLCs, a similar result was expected also for this elementary memory cell (although the number of SLC is not predictable). The expectation was confirmed and the BS morphology is complex (partly because of the presence of a "tail" at \*S2 and \*S5 - Fig. 3(b), Fig. 4) and the BS reconstruction effort in 3D space, as presented in [23], [24], would not be successful. Moreover, the BS morphology should be even more complex, because it was expected that up to 6 stable singularities would appear and redistribution of state space into regions of attraction should be more broken. A surprising finding, however, was that, although the models of memory cells are similar, there is a big difference between them. It rests in the absence of 2 stable singularities S2 and S5 and thus presented memory is only 4-valued (previous memory in [20] was 5-valued), but with up to 9 SLCs present (8 SLC were present in the previous memory in [21]). The fact of changing S2 and S5 to unstable \*S2 and \*S5, was verified by calculation of the trajectories from the surroundings of singularities and by BS cross-section led through both singularities – Fig. 3(b). The author is not familiar with a work dealing with similar sequential circuit at  $R = 0$ , where the character of singularities would be changed. It is therefore probable that this is the first ever reference of a physical sequential circuit where there is no alteration of singularities S–N–S etc.

#### REFERENCES

- [1] J. T. Butler, "Multiple-valued logic", *IEEE Potentials*, pp. 11–14, 1995. [Online]. Available: <http://dx.doi.org/10.1109/45.376636>
- [2] R. Vega, S. Sudirgo, "Multi-valued logic/memory cells and methods thereof", US Patent No. 7548455B2, 2009.
- [3] H. Nan, K. Choi, "Novel ternary logic design based on CNFET," in *Proc. Int. SoC Design Conf. (ISOC 2010)*, 2010, pp. 115–118.
- [4] S. Lin, Y. B. Kim, F. Lombardi, "A novel CNTFET-based ternary logic gate design", in *Proc. 52nd IEEE Int. Midwest Symposium on Circuits and Systems (MWSCAS 2009)*, 2009, pp. 435–438. [Online]. Available: <http://dx.doi.org/10.1109/MWSCAS.2009.5236063>
- [5] J. Nunez, M. Avedillo, J. Quintana, "Evaluation of RTD-CMOS logic gates", in *13th Euromicro Conf. on Digital Syst. Design: Architectures, Methods and Tools*, Spain, 2010, pp. 621–627.
- [6] P. Galajda, "Design of multiple valued RAM memory", in *Proc. of 6. Scientific Conf. EF TU*, Kosice, 1992, pp. 12–15.
- [7] P. Galajda, "Analytical model of the MOS transistor and multiple-valued static RAM simulation", in *Digital signal processing*, Kosice, 1993, pp. 126–129.
- [8] P. Galajda, M. Guzan, V. Spany, "Boundary surfaces of one port memories", in *Proc. 5th Int. Conf. Tesla Millenium*, pp. 131–137, 1996.
- [9] V. Spany, "The simple VA characteristic approximation and the complex analysis of the tunnel diode oscillator", in *Proc. IEEE 55*, pp. 1641–1643, 1967. [Online]. Available: <http://dx.doi.org/10.1109/PROC.1967.5935>
- [10] V. Spany, "Special surfaces and trajectories of the multidimensional state space", in *Proc. Scientific Works of TU of Kosice*, 1978, pp. 123–152.
- [11] V. Spany, L. Pivka, P. Galajda, M. Guzan, P. Kalakaj, A. Sak, "The calculation of symmetrizing voltage in flip flop sensor", in *Radioelectronics, TU*, Kosice, 1994, pp. 22–27.
- [12] V. Spany, "Multistable systems and special surfaces m-dimensional state space", *Elektrotechnicky Casopis*, vol. 33, no. 7, pp. 551–556, 1982. (in Slovak).
- [13] V. Spany, "Boundary surface and model of sequential circuit", in *Proc. Scientific Works*, Kosice, 1985, pp. 103–127.
- [14] V. Spany, L. Pivka, "Boundary surfaces in sequential circuits", *Int. Journal of Circuit Theory and Applications*, vol. 18, no. 4, pp. 349–360, 1990. [Online]. Available: <http://dx.doi.org/10.1002/cta.4490180404>
- [15] P. Galajda, M. Guzan, V. Spany, "The state space mystery with negative load", *Radioengineering*, vol. 8, no. 2, pp. 2–7, 1999.
- [16] P. Galajda, V. Spany, M. Guzan, "The state space mystery with virtual saddle point in memory cell", in *Proc. 6th Int. Conf. Digital Signal Processing and Multimedia Communications (DSP-MCOM 2005)*, Kosice, Slovakia, 2005, pp. 147–150.
- [17] M. Guzan, "Boundary surface and limit cycles of ternary memory by using forward and backward integration", in *Proc. 17th Int. Conf. Electrical Drives and Power Electronics (EDPE 2011)*, Kosice, Slovakia, 2011, pp. 171–175.
- [18] M. Guzan, "Boundary surface of a ternary memory in the absence of limit cycles", in *Proc. 22nd Int. Conf. Radioelektronika*, Brno, Czech republic, 2012, pp. 1–4.
- [19] M. Guzan, R. Bucko, "Morphological complexity of state space quaternary memory", *Electrical Engineering and Informatics II, Proc. Faculty of Electrical Engineering and Informatics of the Technical University of Kosice*, 2011, pp. 518–521.
- [20] M. Guzan, "Boundary surface of 5-valued memory", *Journal of Engineering*, p. 7, 2013. [Online]. Available: <http://dx.doi.org/10.1155/2013/626824>
- [21] V. Spany, "The expression of the non-linear characteristics by means of absolutes values", *Slaboproudy obzor*, vol. 40, no. 7, pp. 354–356, 1988. (in Slovak).
- [22] P. Galajda, M. Guzan, V. Spany, "The control of a memory cell with the multiple stable states", in *Proc. 21th Int. Conf. Radioelektronika*, Brno, Czech Republic, 2011, pp. 211–214. [Online]. Available: <http://dx.doi.org/10.1109/RADIOELEK.2011.5936469>
- [23] M. Guzan, B. Sobota, "Boundary surface of multiple-valued memory in 3D", in *Sekel Int. Conf. teachers electrotechnics*, Bratislava, 2012, pp. 75–80. (in Slovak).
- [24] B. Sobota, "3D modelling of Chua's circuit boundary surface", *Acta Electrotechnica et Informatica*, vol. 11, no. 1, pp. 44–47, 2011. [Online]. Available: <http://dx.doi.org/doi:10.2478/v10198-011-000>